

Interacting biological and electronic neurons generate realistic oscillatory rhythms

Attila Szűcs,^{CA} Pablo Varona, Alexander R. Volkovskii, Henry D. I. Abarbanel,¹ Mikhail I. Rabinovich and Allen I. Selverston

Institute for Nonlinear Science, University of California San Diego, 9500 Gilman Drive, La Jolla, CA 92093-0402; ¹Department of Physics and Marine Physical Laboratory, Scripps Institution of Oceanography, University of California San Diego, La Jolla, CA 92093-0402, USA

^{CA}Corresponding Author

Received 22 October 1999; accepted 9 December 1999

Published online by xx xxxx 2000

Acknowledgements: Partial support for this work comes from the US Department of Energy, Office of Basic Energy Sciences, Division of Engineering and Geosciences, under grant DE-FG03-90ER14138 and DE-FG03-96ER14592.

Small assemblies of neurons such as central pattern generators (CPG) are known to express regular oscillatory firing patterns comprising bursts of action potentials. In contrast, individual CPG neurons isolated from the remainder of the network can generate irregular firing patterns. In our study of cooperative behavior in CPGs we developed an analog electronic neuron (EN) that reproduces firing patterns observed in lobster pyloric CPG neurons. Using a tuneable artificial synapse we

connected the EN bidirectionally to neurons of this CPG. We found that the periodic bursting oscillation of this mixed assembly depends on the strength and sign of the electrical coupling. Working with identified, isolated pyloric CPG neurons whose network rhythms were impaired, the EN/biological network restored the characteristic CPG rhythm both when the EN oscillations are regular and when they are irregular. *NeuroReport* 11:1–7 © 2000 Lippincott Williams & Wilkins.

Key words: Electronic neuron; Electronic synapse; Oscillatory rhythm; Pyloric neurons; Regularization; Synchronization

INTRODUCTION

Central pattern generators (CPGs) are widely studied systems of rhythm generation in small neuron assemblies [1]. The regularity and stationarity of the oscillatory patterns generated by a small number of interacting neurons is noteworthy, especially in light of evidence that such networks are composed of individual neurons which can oscillate chaotically when observed in isolation. Indeed, CPG neurons with their synaptic inputs blocked have been shown to express chaotic firing patterns [2–6]. Regular rhythm generating neurons called pacemakers are commonly believed to be fundamental parts of the CPGs, initiating the main oscillation [7]. A pacemaker neuron or group may be required to synchronize all other neurons and control joint rhythms because of the differences in the properties of individual neurons.

The stomatogastric ganglion (STG) of crustaceans is a well understood nervous system [8]. It contains the pyloric CPG that generates a highly regular and repetitive motor pattern resulting from interactions between 14 neurons. In this system the anterior burster (AB) neuron is one of the main pacemaker elements, having a central role in organizing the rhythm. The two electrically coupled pyloric dilator (PD) neurons fire in-phase with the AB forming a triplet of pacemaker neurons. The robustness and uniformity of the

oscillation initiated by AB makes it difficult to manipulate or interact with the rhythm and investigate the role of individually irregular PDs in the pattern generation.

Based on our non-linear analysis of experimental data from isolated pyloric neurons, we have developed a simple analog electronic model of CPG neurons capable of reproducing the observed firing patterns. The 'electronic neuron' (EN) was connected to the PD cells using an artificial synapse, thus forming a mixed circuit. This approach allowed us to dynamically interact with the biological neurons rather than stimulating them using response-independent current commands. In this fashion we have shown that the regular, natural rhythm of the PD in the intact network is restored when interacting with the ENs. This occurs both when the EN is behaving regularly and when it is set into a state of chaotic oscillations.

MATERIALS AND METHODS

Preparation and electrophysiology: The stomatogastric nervous system (STNS) of the spiny lobster *Panulirus interruptus* L. was dissected and prepared as described earlier [9]. Briefly, the STG, the esophageal ganglion and the two commissural ganglia with the interconnecting nerves were separated from the stomach and pinned in a Sylgard-lined Petri dish containing standard *Panulirus* physiologi-

cal saline [3]. The STG was perfused separately from the rest of the STNS using a vaseline chamber. Picrotoxin (PTX; 7.5 μ M) was used to block glutamatergic synaptic transmission and isolating the pyloric pacemaker group from other pyloric neurons. Nerve cells were identified by comparing intracellular signals with extracellular burst patterns monitored simultaneously from output motor nerves. Partial isolation of the two PD neurons was performed by photoinactivating the presynaptic AB neuron [10]. The membrane potential of the cells was measured with Neuroprobe 1600 current-clamp amplifiers (AM-Systems). The PD neuron which we connected to the electronic neuron was impaled with two microelectrodes filled with 3M KCl and with resistances of 10-15 M Ω . One of these was used to monitor the membrane potential, while the other served as a current passing electrode. This method allowed us to avoid any problems arising from imperfect bridge balancing or non-linearities of the current passing electrode. A total of 198 trials were performed on nine preparations.

Electronic neuron and synapse: We have designed and built a three degree of freedom analog electronic circuit realization of a mathematical model of bursting neurons. The model was suggested by the work of Hindmarsh and Rose [11]. It uses a polynomial representation of the dependence of ion currents on the membrane potential according to the following differential equations:

$$\dot{x} = 4y + \frac{3x^2}{2} - \frac{x^3}{4} - 2z + \varepsilon, \quad \dot{y} = \frac{1}{2} - \frac{5x^2}{8} - y,$$

$$\dot{z} = \mu(-z + 2x + 6.4)$$

where x is the membrane potential, y and z are 'fast' and 'slow' internal variables, ε represents the external currents, and μ is the time constant of the slow variable. Both ε and μ are tuneable parameters. The HR model captures the most important firing/bursting modes of real CPG neurons [12]. This model, however, generates spikes with too large an amplitude relative to the depth of interburst hyperpolarization. To make this ratio more realistic we used an additional nonlinear amplifier which reshaped the output of the HR model neuron and made the membrane potential oscillation more similar to that of bursting pyloric neurons (compare Fig. 1A, PD trace with Fig. 2A, EN trace). The EN, connected bidirectionally to the PD, was able to receive and process incoming signals in the same fashion as biological neurons receiving synaptic inputs. This functionality came from an additional electronic circuit simulating an electrotonic synapse. The potential difference between the EN and the biological neuron was measured, and a current signal proportional to the difference was generated. This current was fed back to the EN and connected to the current input of the intracellular amplifier with opposite polarity. The amplitude and sign of the current depended on the actual potential difference and a conductance parameter, set by the experimenter.

Data acquisition and analysis: The extra- and intracellular signals were acquired at 10 kS/s rate by the Axoscope 7.0 program running on a PC. Raw membrane potential data were visually inspected, and detailed quantitative

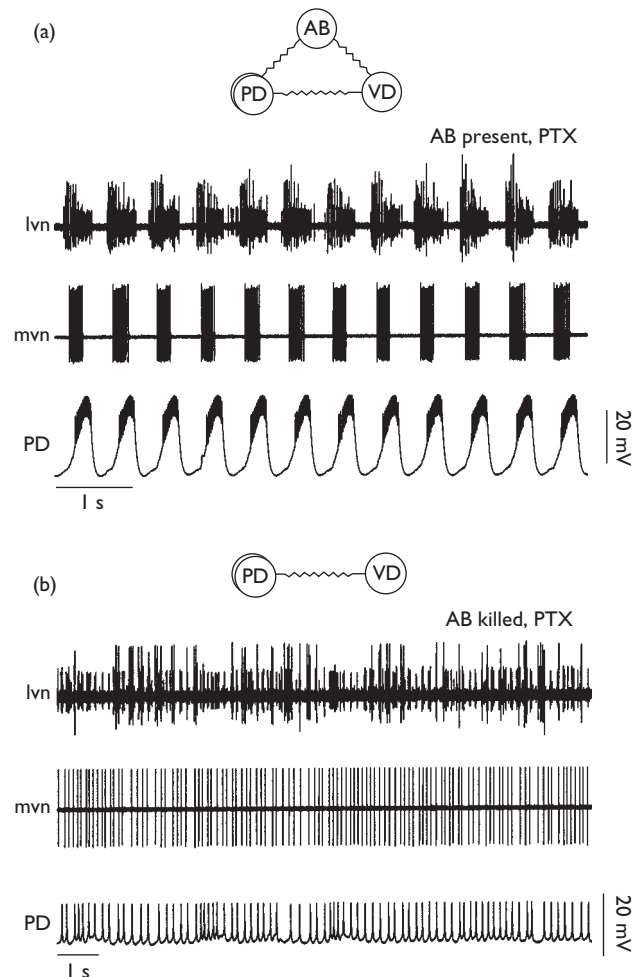


Fig. 1. Comparison of the activity patterns of pyloric neurons with the main pacemaker neuron AB present and shortly after photoinactivation of AB. Glutamatergic transmission was blocked by PTX. (a) Spikes of the LP (large), PD and PY (small) neurons appear in the extracellular recording from the lateral ventricular nerve (lvn). Activity of the VD neuron was monitored from the medial ventricular nerve (mvn). The bottom trace shows the firing pattern of the PD neuron (intracellular). (b) Disruption of the pyloric oscillation shortly after killing the AB neuron. PD and VD neurons were firing tonically; large spikes in the lvn recording indicate irregular bursts in LP.

analysis was performed using spike arrival times. The time derivative of the intracellular time series was used to detect spike events, and interspike-interval (ISI) sequences were constructed for each train. First-order return maps of the ISIs were used as a graphical tool characterizing the overall dynamics and the regularity of the firing patterns. The spike-density function (SDF) [13] was used to characterize modulations of the firing patterns and to detect correlations between simultaneous spike trains. The SDF technique allowed us to obtain firing rate as a continuous function of the elapsed time [14]. An SDF was constructed by convolving the time of each spike event with a Gaussian-function (kernel) of unit area and fixed half-width, typically 0.2 s here. The Fourier transform of the spike density functions was used to detect any periodicities

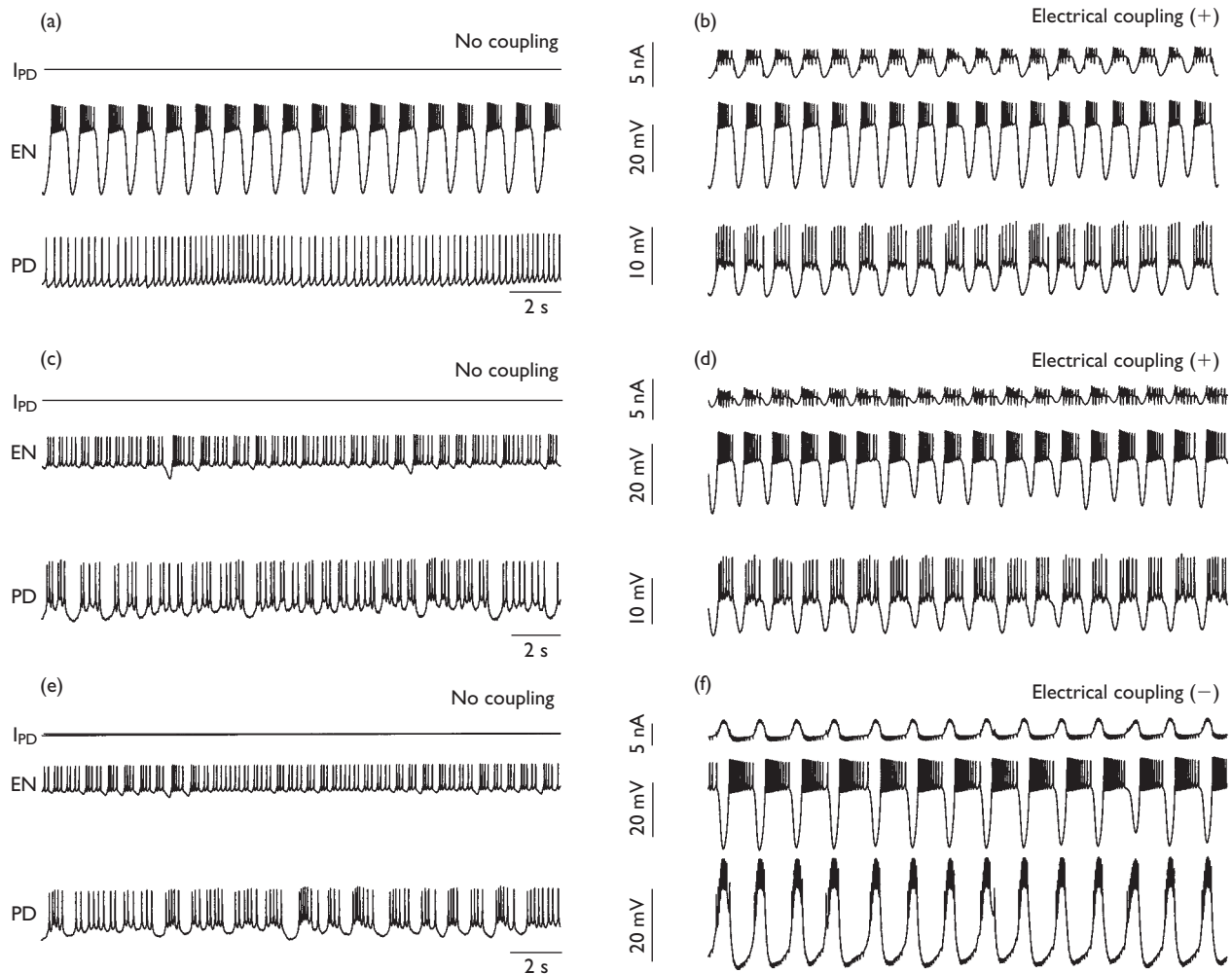


Fig. 2. Comparison of the intracellular firing patterns of the EN and the PD. Left panels: neurons disconnected, synapse off; right panels: electrotonic coupling. I_{PD} in each panel is the current flowing into PD through the electronic synapse. (a) Periodic bursting in EN with tonic spiking in PD (AB killed). (b) Synchronous bursting in EN and PD after switching on the electrical connection. (c) Chaotic firing in EN with irregular spiking in PD, no coupling. (d) Generation of the bursting pattern in the EN–PD mixed network after coupling via an electrotonic synapse. (e) Same as in C. (f) Periodic antiphase bursting in EN and PD neuron with negative conductance connection.

in the firing patterns. Phase portraits were constructed by plotting the SDF of one neuron against that of the other. This graphical tool revealed cross-correlations between neurons recorded simultaneously.

RESULTS

Intact and reduced pyloric network: The pyloric pacemaker group of the lobster consists of four electrotonically coupled neurons: AB, two PDs and the VD neuron [7]. There are strong symmetrical connections between AB and the PD neurons and weaker rectifying connections between the AB and VD [15]. These nerve cells express a regular oscillatory pattern in the intact preparation (Fig. 1A). Picrotoxin, while blocking all glutamatergic synaptic inputs and functionally isolating the pacemaker network, had little effect on the frequency or amplitude of the ongoing oscillation. In contrast, photoinactivation of the main pacemaker neuron AB led to complete disruption of the pyloric rhythm. Removal of AB led to cessation of the bursting

activity in PD neurons and in VD (Fig. 1B). Initially, after photoinactivation the PD expressed irregular spiking behavior that evolved after about 1 h into irregular bursting. The irregular bursting pattern remained for the lifetime of the preparation.

Connecting EN to isolated PD neurons—regular bursting: Because of the flexibility of our analog circuit, we could generate a broad range of firing/bursting patterns in EN by tuning the ϵ and μ parameters. In the experiments reported here, we first generated regular bursting in the EN and connected it to the PD. Essentially the EN behaved as a new pacemaker neuron: it acted as a replacement for the AB in the network. Prior to connection, we adjusted the parameters of the EN to obtain oscillation similar in amplitude (30–40 mV) and frequency (1.2–1.8 Hz) to that seen in AB. Electrotonic coupling shifted the firing pattern of PD from tonic spiking to bursting (Fig. 2A,B). The slow-wave components of the oscillations synchronized, while

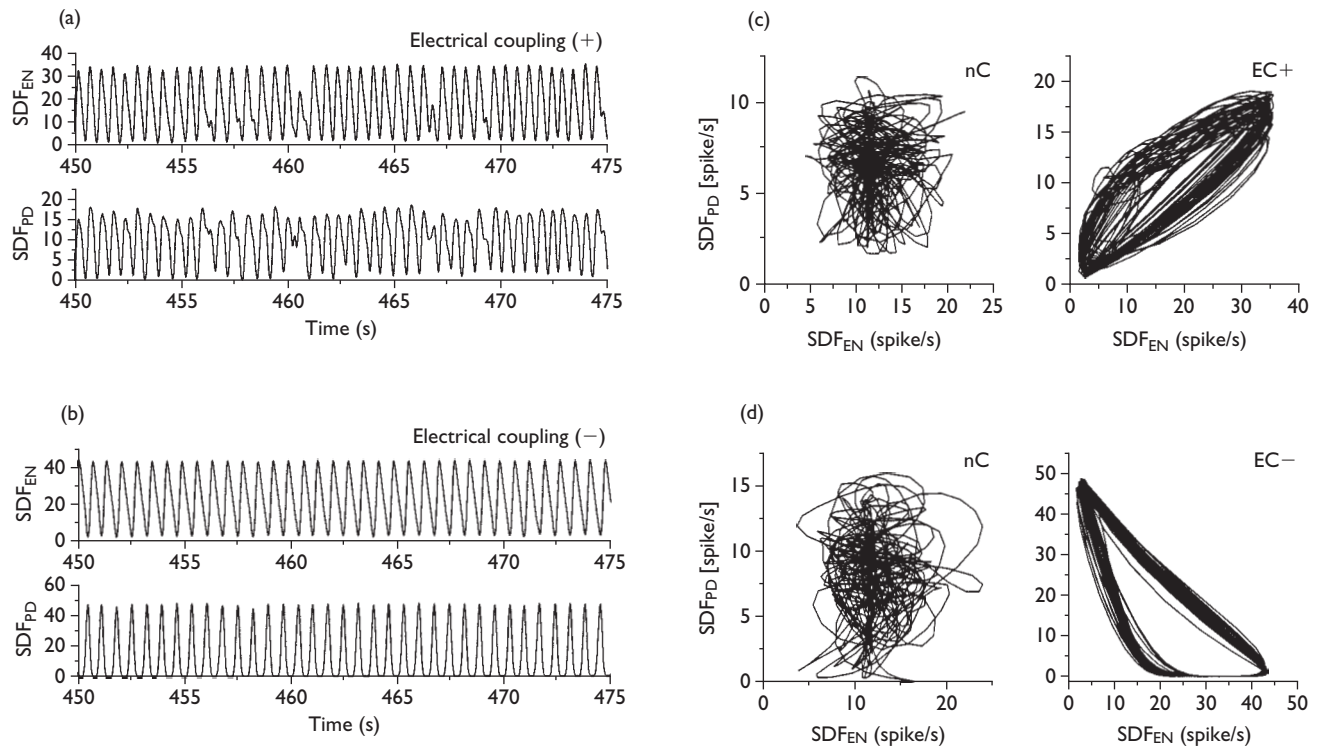


Fig. 3. Spike density functions (SDFs) calculated from the spike trains of coupled EN and PD neurons. **(a,b)** 25 s long sections of the SDFs with positive and negative conductance synaptic connections, respectively. The functions exhibit oscillating firing patterns in both neurons. Variation of the SDF is smaller when using negative conductance coupling, indicating strong mutual regularization. **(c)** Phase-portrait graphs before (nC, no connection) and after (EC+) connecting the EN to PD via positive conductance synapse. **(d)** Same graphs with negative conductance (EC-) connection.

single spikes in EN and PD did not. The bursting pattern of PD induced by the electrotonic coupling resembled that in the intact pyloric pacemaker network. Monitoring activity of the output nerve *Ivn* showed that the burst pattern of the postsynaptic neuron LP was also synchronized with the EN-PD pair, leading to a partial restoration of the pyloric rhythm. Inserting EN as a regular, periodic bursting element into the impaired neuronal network induced a new overall oscillation, quite similar to the original pyloric rhythm.

Connecting chaotic electronic and pyloric neurons: The EN is also able to generate chaotic patterns. In this case, no periodic spike patterns were produced by the EN. Figure 2C shows the similarities of the time series of chaotic EN and the isolated PD neurons before coupling, both firing in an irregular manner. Non-linear analysis using the method of false nearest neighbors [16] of the bursting pattern of the free-running PD neuron indicated high-dimensional (up to seven) chaotic dynamics. Remarkably, electrotonic coupling dramatically altered the firing patterns of both EN and PD. Synchronized bursting appeared immediately after coupling the electronic model to the pyloric cell (Fig. 2D). The frequency of the bursting was close to that seen in the intact pyloric network. As a consequence of this high-degree of synchronization, the synaptic current being injected into PD showed only minor fluctuations.

To approximate a graded inhibitory synapse, we used negative conductance coupling between the neurons.

Although the synaptic current remained a linear function of the membrane potential difference, negative conductance coupling was in some aspects similar to a mutual inhibitory chemical connection but without delay, threshold or non-linear properties. The effect observed upon coupling in the chaotic EN to the PD was even more dramatic (Fig. 2F), although the neurons were bursting in anti-phase. A clean periodic bursting pattern appeared after initiating this coupling, and the time series of the PD was virtually indistinguishable from that seen in the intact CPG. Inhibitory postsynaptic potentials from EN were apparent in the membrane potential of PD, and strong rebound plateaus followed the hyperpolarized states. These data clearly demonstrate that regular and robust oscillatory patterns characteristic of the intact pyloric CPG can be achieved by simply coupling the intrinsically irregular/chaotic EN to the PD neuron. As a control, we performed experiments with constant negative current injection into the PD neuron and with unidirectional coupling between EN and PD. In that case, we did not observe regularization of PD. Regularization appears only when the PD is connected bidirectionally to the EN.

Analysis of spike time data: Spike density functions clearly showed the most prominent features of the EN-PD interaction and revealed new details about this process. The SDFs of the uncoupled neurons, when both were firing in an irregular pattern, were aperiodic and random-like (not shown). The corresponding phase-portrait possesses

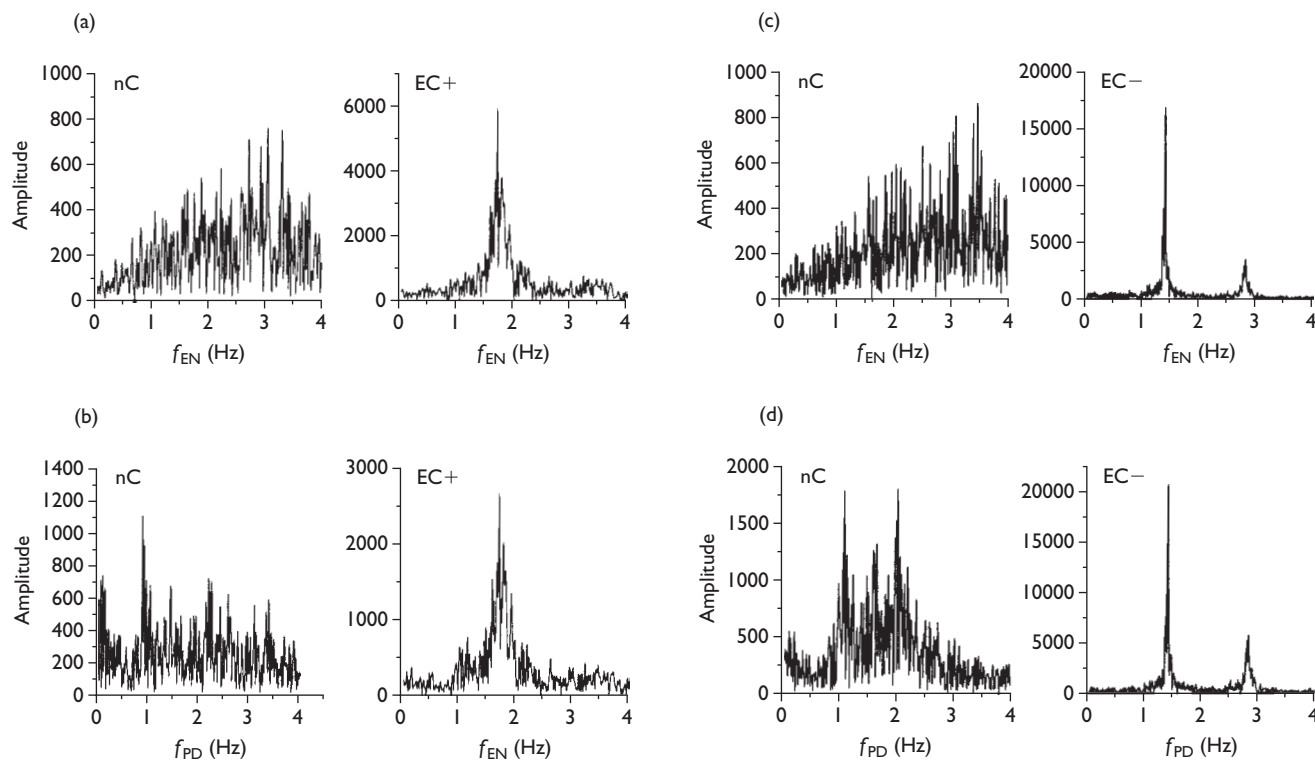


Fig. 4. Fourier transforms of the spike density functions of free-running and coupled EN and PD neurons. The spectra were calculated from simultaneous sections of the SDFs. (a,c) EN; (b,d) PD. Broad band, 'noisy' Fourier spectra imply irregular dynamics of both the EN and the PD when disconnected (nC). A very weak periodicity with 1 Hz frequency can be detected in the free-running PD. Clear peaks appear as a consequence of periodic bursting behavior when using a positive (EC+) or negative (EC-) conductance synapse.

no apparent structure or orientation (Fig. 3C, left). Positive electrotonic coupling led to synchronized oscillations in the SDF (Fig. 3A) and diagonal trajectories in the phase-portrait (Fig. 3C, right). SDFs in negative conductance coupling experiments exhibited a similar behavior. SDFs of both EN and PD are precisely periodic (Fig. 3B), and the phase-portrait consists of a tight trajectory with negative slope (Fig. 3D, right). The Fourier transforms of the SDFs of uncoupled irregular EN and PD neurons had a broad band 'noisy' distribution characteristic of chaotic dynamics (Fig. 4). Sharp peaks in the Fourier spectra appear as a consequence of periodic bursting when the neurons were connected. The frequency of the oscillation (1.8 and 1.4 Hz with positive and negative coupling, respectively) was close to the pyloric rhythm observed in the intact preparation.

Dependence of the effects on coupling strength: The experiments involved systematic scanning of the parameters of the EN, tuning the shape of the oscillation, as well as changing the synaptic strength between the electronic and pyloric neuron. ISI sequences measured from a long-term experiment and return maps of the same data are shown in Fig. 5. The intrinsically chaotic EN was coupled to an irregular PD neuron via positive conductance electrotonic synapse. The 'burstiness' of the firing patterns depended on the strength of the connection. Weak coupling resulted in minor changes in the PD, whereas strong coupling resulted in clear burst activity, with a bimodal ISI distribu-

tion. The triangular structure of the ISI return map shown in Fig. 5C and D is characteristic of periodically bursting neurons. This pattern emerged after electrically coupling an intrinsically chaotic EN to the isolated PD. Negative conductance coupling had a stronger regularizing effect on the firing of the neurons in all cases. The magnitude of the changes in the ISI pattern of the EN was a function of the connection strength as well as the firing pattern set prior to the coupling. Switching off the electrotonic connection commonly led to quick restoration of the irregular firing or bursting pattern in PD.

DISCUSSION

Several implementations of neural models in electronic circuits have been used to capture aspects of neuronal function and organization in what recently has been called neuromorphic systems [17,18]. Mixed circuits consisting of biological neurons and electronic devices are particularly useful in studying small neural systems such as those of CPGs. Only in very few instances have analog implementations of model neurons and synapses actually been used to interact with biological cells. An analog network of coupled subthreshold oscillators was connected to olivary neurons in Yarom's work [19] and the mechanisms of synchronized neural oscillations were investigated. In another study Le Masson and coauthors used BiCMOS implementations of complex, multiparameter Hodgkin-Huxley models [20]. Several features of the neural function of stomatogastric neurons as well as thalamocortical cells

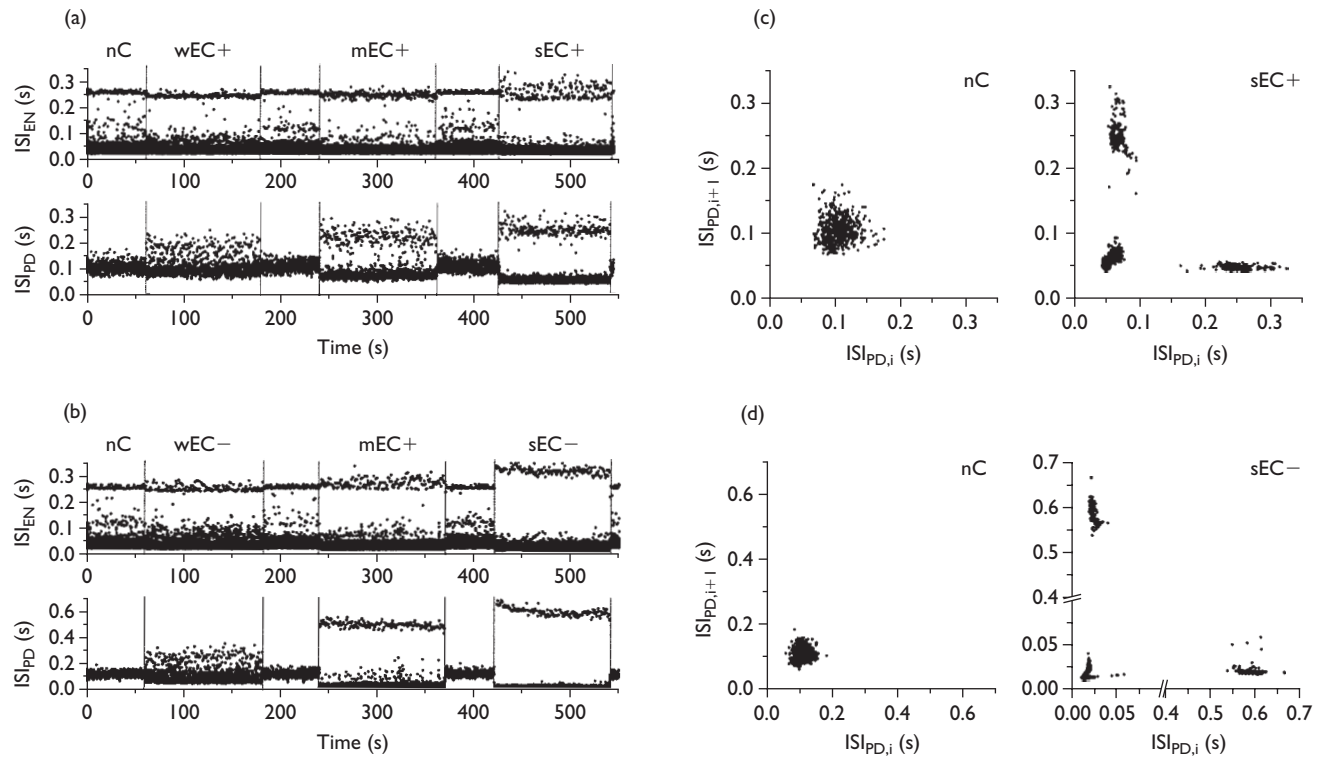


Fig. 5. Interspike-interval sequences and return maps. **(a,b)** Time vs ISI graphs calculated from 550 s long spike trains. Vertical lines mark the onset and release of the electrical connection with various strength (wEC+/-: weak, mEC+/-: moderate and sEC+/-: strong). **(c,d)** ISI return maps constructed from various parts of the corresponding ISI sequences of the PD neuron. A diffuse cloud of points indicates highly irregular spiking in the isolated PD. The triangular form appears as a consequence of burst generation when using strong coupling (sEC+ and sEC-).

were reconstructed by these electronic models. A similar approach has been utilized by constructing artificial synaptic connections between existing biological neurons using advanced computer techniques [21,22]. Clearly, response-dependent stimulation of biological neurons have proven a fruitful method to study details of cellular excitability or network dynamics.

In our work we used a simplified, yet realistic, electronic model of a stomatogastric neuron. Instead of making an effort to simulate all ionic conductances contributing to the membrane potential of the living lobster neurons, we built a three-variable analog circuit. Previously we have shown that computational models of Hindmarsh-Rose type neurons reproduce several aspects of the neural function of spiking/bursting neurons [12]. These mathematical models exhibited various firing/bursting patterns and bifurcations similar to those seen in living stomatogastric neurons, when coupled in dynamic clamp experiments [22].

In this note we have presented evidence that two different irregular neurons, one biological and one electronic, are able to produce regular rhythm, when coupled electrically over a wide range of coupling strengths. Regular rhythms can be produced by intrinsically nonregular neurons. These results also suggest that it is not necessary to reproduce all of the biological aspects of the operation of nerve cells to address issues of communication and cooperation among oscillating neurons in CPG-like networks. The full mechanism of the observed regularization phenomenon is not

clearly understood yet and requires additional investigation. However, from the dynamical systems theory point of view such behavior is plausible: coupling two different chaotic elements in fact means the creation of a new dynamical system with new types of possible behavior. In our case the slow bursting dynamics suppresses the chaotic instability of spikes and leads to regular synchronized oscillations.

CONCLUSION

We have shown here the broad value of a 'mixed technology' in the investigation of important physiological problems related to the dynamics of small neural networks. The interaction of an EN with groups of living neurons provides the potential for changing the connectivity and topology of neural networks. It also allows better understanding of the roles of intrinsic and synaptic properties of neurons in rhythm generation or information processing. The noteworthy simplicity of our EN suggests that these circuits may be used as replacement neurons in other CPGs that appear as control systems in more complex organisms. The application of these mixed systems to robotics may also be possible.

REFERENCES

1. Marder E. *Neuroscientist* 3, 295-302 (1997).
2. Bal T, Nagy F and Moulins M. *J Comp Physiol* 163, 715-727 (1988).
3. Elson RC, Huerta R, Abarbanel HDI et al. *J Neurophysiol* 82, 115-122 (1999).

4. Rabinovich MI and Abarbanel HDI. *Neuroscience* **87**, 5–14 (1998).
5. Hayashi H and Ishizuka S. *J Theor Biol* **156**, 269–291 (1992).
6. Mpitsos GJ, Burton RM, Creech HC and Soinila SO. *Brain Res Bull* **21**, 529–538 (1988).
7. Marder E and Calabrese RL. *Physiol Rev* **76**, 687–717 (1996).
8. Harris-Warrick RM, Marder E, Selverston AI and Moulins M. *Dynamic Biological Networks, The Stomatogastric Nervous System*. Cambridge MA, MIT Press, 1992.
9. Mulloney B and Selverston AI. *J Comp Physiol* **91**, 1–32 (1974).
10. Selverston AI and Mulloney B. *J Neurophysiol* **44**, 1102–1121 (1980).
11. Hindmarsh JL, and Rose RM. *Proc Roy Soc Lond B* **221**, 87–102 (1984).
12. Rabinovich MI, Abarbanel HDI, Huerta R *et al.* *IEEE Trans Circ Systems* **44**, 997–1005 (1997).
13. Szűcs A. *J Neurosci Methods* **81**, 159–167 (1998).
14. Paulin MG. *Biol Cybern* **66**, 525–531 (1992).
15. Johnson BR, Peck JH, and Harris-Warrick RM. *J Comp Physiol* **172**, 715–732 (1993).
16. Abarbanel HDI. *Analysis of Observed Chaotic Data*. New York: Springer-Verlag, 1996.
17. Douglas R, Mahowald M and Mead C. *Ann Rev Neurosci* **18**, 255–281 (1995).
18. Mead C. *Analog VLSI and Neural Systems*. Reading, MA: Addison-Wesley, 1989.
19. Yarom Y. *Neuroscience* **44**, 263–275 (1991).
20. Le Masson S, Laflaquière A, Bal T and Le Masson G. *IEEE Trans Biomed Eng* **46**, 638–645 (1997).
21. Sharp AA, O'Neil MB, Abbott LF and Marder E. *Trends Neurosci* **16**, 389–394 (1993).
22. Elson RC, Selverston AI, Huerta R *et al.* *Phys Rev Lett* **81**, 5692–5695 (1998).